

# Estimation of melanin content in iris of human eye: prognosis for glaucoma diagnostics

Alexey N. Bashkatov<sup>1</sup>, Ekaterina V. Koblova<sup>2</sup>, Elina A. Genina<sup>1</sup>, Tatyana G. Kamenskikh<sup>2</sup>, Leonid E. Dolotov<sup>1</sup>, Yury P. Sinichkin<sup>1</sup>, Valery V. Tuchin<sup>1</sup>

<sup>1</sup>Department of Optics and Biomedical Physics of Saratov State University, 83, Astrakhanskaya str., Saratov, 410012, Russia

<sup>2</sup>Ophthalmology Department of Saratov State Medical University, 112, B. Kazach'ya str., Saratov, 410012, Russia

## ABSTRACT

Based on the experimental data obtained *in vivo* from digital analysis of color images of human irises, the mean melanin content in human eye irises has been estimated. For registration of the color images a digital camera Olympus C-5060 has been used. The images have been obtained from irises of healthy volunteers as well as from irises of patients with open-angle glaucoma. The computer program has been developed for digital analysis of the images. The result has been useful for development of novel and optimization of already existing methods of non-invasive glaucoma diagnostics.

**Keywords:** iris, melanin content, glaucoma, digital image analysis

## 1. INTRODUCTION

Knowledge of tissue optical properties is important for development of theoretical models describing the light propagation within tissues (including a human eye iris). These models can be used when designing laser therapy and diagnostic techniques, or interpretation of the data of spectrophotometric measurements. There are numerous papers describing the methods of determination of optical properties of many types of tissues.<sup>1</sup>

Recently some diagnostic criteria of dystrophic, degenerative and inflammatory diseases of an eye iris have been based on descriptive, relative and, in many respects, subjective criteria to which the discoloration of an iris of the eye is also referred.<sup>2-7</sup> Now the eye iris classification is based on the data of iridochromoscopy, iridochromophotography, and biomicroscopy in polarized light.<sup>2-8</sup> Objective criteria of inflammatory and degenerative changes can be obtained from data of the fluorescent angiography. Unfortunately, the method is invasive and cannot be applied to all patients. Iris coloration depends mostly on the amount and depth of location of melanin located in the forefront mesodermal part of the iris.<sup>4,5,7,8</sup> The quantitative assessment of melanin content in an iris can be used as an objective criterion in investigating the series of pathological conditions.<sup>2,4,7,8</sup> Besides, the objective data could be supplement to the existing classifications of iris types.

In this study, we present a method for estimation of melanin content in eye iris with digital analysis of color images of the eye iris.

## 2. STRUCTURE AND PROPERTIES OF THE HUMAN EYE IRIS

Figure 1 shows the transverse (horizontal) section of an eyeball. The eye iris is forefront of choroid of the eye. The iris has the form of a plate with slightly elliptical shape. Peripheral edge of the iris (its root) is merged with the ciliary body and the trabecular meshwork. The iris is 12-12.5 mm in diameter with a circumference of 36-37 mm.<sup>4,9,10</sup> The forefront surface of the iris can be separated on the two zones: the pupil zone (1-2 mm wide) and the ciliary zone (3-4 mm wide). The separation line corresponds to plexus of small arteries, which form a small arterial iris circle. The distance between

---

[bash@optics.sgu.ru](mailto:bash@optics.sgu.ru)

the separation line and edge of eye pupil is about 1.5 mm.<sup>9</sup> Iris thickness is not everywhere equal. The thickness has maximal value (up to 480-550  $\mu\text{m}$ ) in the area of the small arterial circle, and minimal value was observed in ciliary zone - up to 350  $\mu\text{m}$ .<sup>11</sup> Eye pupil has also very different size. For children the pupil diameter is minimal (up to 2 mm), in the young age the pupil diameter is maximal (about 4 mm), and in the old age the pupil diameter decreases again.

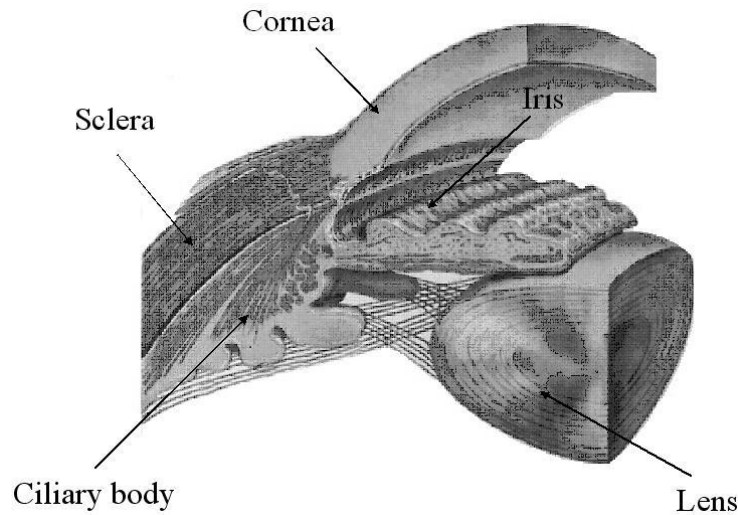


Fig. 1. The transverse (horizontal) section of eyeball

Structurally, the iris contains two different layers. The iris thin innermost layer is called the iris pigment epithelium (IPE) and consists of a compact array of opaque cells. The outermost layer is referred to the iris stroma, which contains more loosely arranged cells, including melanocytes that synthesizes the pigment.<sup>4-6,12,13</sup> The iris structure is illustrated in figure 2. According to electronic microscopy, basic cellular elements of the stroma layer are fibroblasts, melanocytes and a network of collagen fibrils.<sup>4-6,12</sup> Diameter of collagen fibrils in iris stroma is 60 nm and its axial periodicity is 50-60 nm.<sup>5</sup> Size of the iris melanocytes is about 100  $\mu\text{m}$  and the cells are filled by very small melanin particles.<sup>5,11-13</sup> Structurally, the stroma can be subdivided in two sublayers: the mesodermal upper and deep sublayers. In the upper sublayer of stroma (in ciliary zone) melanocyte conglomerations form the pigmentary spots, so-called nevuses.<sup>4-6,12</sup>

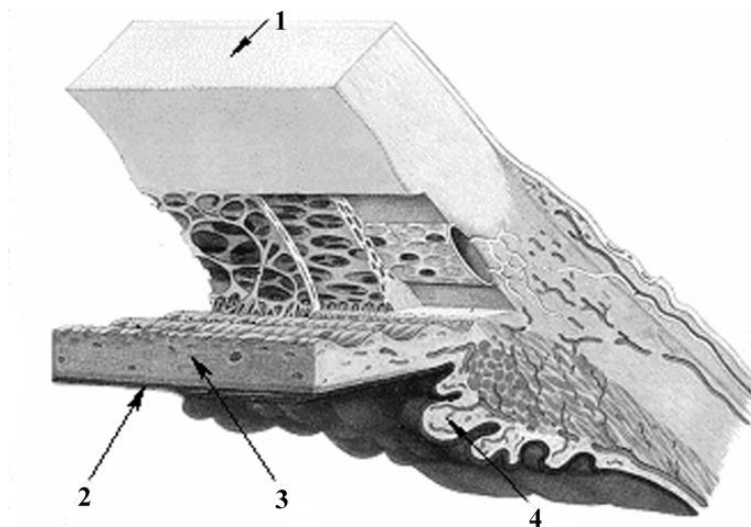


Fig. 2. The eye iris structure: 1 - the cornea; 2 - the iris pigment epithelium (IPE); 3 - the iris stroma; 4 - the ciliary body  
Iris vessels are localized within the iris stroma. The vessels include large vessels (arterioles and venules) and capillaries.<sup>6</sup>

In the depth of the iris stroma, nearly the iris root (in area of the eye trabecular meshwork), iris arteries and venules form large arterial circle of the iris. From this circle, radial vessels with a diameter smaller than the diameter of the vessels of the large arterial circle go to the eye pupil.<sup>9</sup> Size of the large iris vessels (arterioles) is 50-100  $\mu\text{m}$ . Precapillaries have diameter 14-16  $\mu\text{m}$ , and capillaries 3-12  $\mu\text{m}$ . Diameter of venules is 12-100  $\mu\text{m}$ .<sup>14</sup> Unfortunately, blood content in eye iris has been investigated not enough, however, for choroid the volume fraction of blood are known. Hammer and Schweitzer<sup>15</sup> found the volume fraction as 20%, Delori and Pflibsen<sup>16</sup> estimated the fraction as 50%, and Preece and Claridge<sup>17</sup> reported that the choroid blood volume fraction ranged from 50 to 80%. Since iris is forefront of the eye choroid then it is necessary to expect, that blood content in the iris can be taken from approximately 30 to 70%.

From the iris structure, there are three principal elements that contribute to its color.<sup>18</sup> One is the pigment in the IPE, which is black in irises of all colors. Another is the melanin content in the iris stroma, which is the primary cause of color variations among different irises.<sup>17</sup> Brown irises have a large amount of melanin, which absorb much of the incoming light especially at short wavelengths. For blue irises which have low melanin content in the stroma, long-wavelength light penetrates the stroma and is absorbed in the IPE, while the short-wavelength undergoes Rayleigh scattering and reflection. Green and hazel irises are products of moderate amounts of melanin. Thus, the spectrum of iris colors basically results from varying amounts of the stroma melanin. However, blood of the stromal vessels also contributes in forming iris color, especially in short-wavelength spectral range. The third structural component that influences color is the cellular density of the iris stroma. For example, in an area of low density, little light is reflected by the semi-transparent stroma, so it shows the black color of the IPE, and, on the contrary, in an area of high density light does not penetrate IPE and backreflected by the iris stroma.

Melanin synthesis occurs in special organoids - melanosomes, and then a transformation into enzymatic-inert pigmentary granules takes place. In accordance to its chemical composition the pigment is a combination of sulfur-containing pheomelanin and sulfur-free eumelanin, and the content of the pheomelanin produced by melanocytes at early and mature cells age is dominating (up to 99%). At cells ageing there is a eumelanin contents dominating.<sup>19-23</sup> Melaninous granules in the residual bodies laying in the stroma's back part are identical in size and form to the pigment granules of the pigmentary epithelium covering the iris back surface. It should be noted that melanin's granules size enclosed in the residual bodies located in forefront of iris stroma is equal to melanin granules size in melanocytes.<sup>4-6</sup> In Fig. 3 the extinction coefficient spectra<sup>24</sup> of pheomelanin and eumelanin are presented.

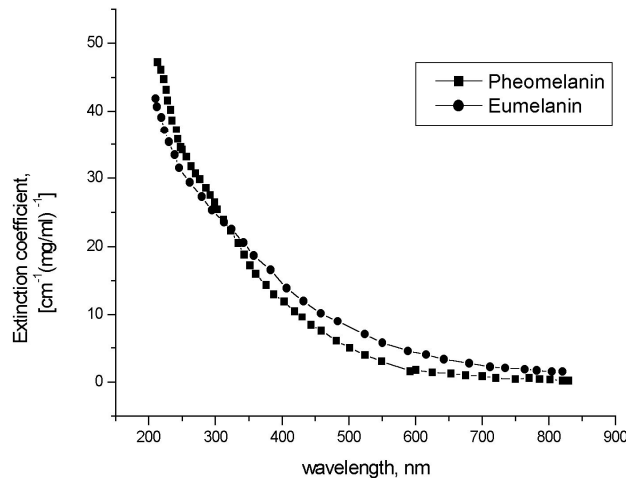


Fig. 3. Extinction coefficient spectra of melanins<sup>24</sup>

Since structure and function of iris pigment epithelium is very similar to structure and function of retinal pigment epithelium then we can assume that optical properties of these tissues are also very similar. Hammer et al.<sup>25</sup> measured the optical properties of retinal pigment epithelium earlier and we have used the data in our calculation. Figure 4 and 5 show the optical properties of retinal pigment epithelium obtained by digitization of the data presented by Hammer et al.<sup>25</sup>

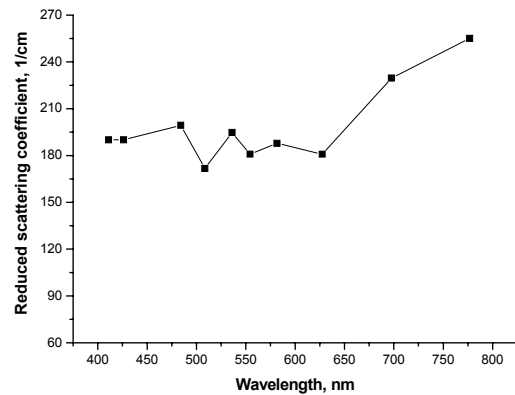
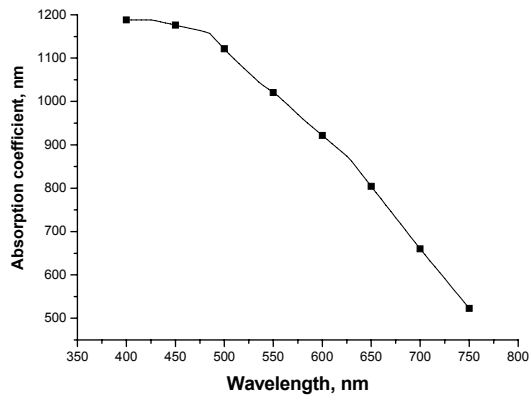


Fig. 4. The absorption properties of retinal pigment epithelium<sup>25</sup> Fig. 5. The scattering properties of retinal pigment epithelium<sup>25</sup>

### 3. MATERIALS AND METHODS

Estimation of melanin content in human irises using experimental data obtained *in vivo* from digital analysis of color images of the irises has been performed. For estimation of scattering properties of iris stroma, the reflectance measurements of rabbit's vitiligo irises have been performed. The reflectance measurements were carried out using commercially available optical multichannel spectrometer LESA-6med (BioSpec, Russia). Figure 6 shows a scheme of the experimental setup.

As a light source a 250 W xenon arc lamp with filtering of the radiation in the spectral range from 400 to 700 nm has been used in the measurements. Light was delivered to the iris and collected from the tissue using the originally designed optical probe, which consists of two optical fibers. Both fibers have 400  $\mu\text{m}$  in core diameter and a numerical aperture of 0.2. The fibers have been enclosed in aluminum jacket (8-mm outer diameter) to provide a fixed distance between the fibers and the tissue surface. The central fiber has been placed in perpendicular to iris surface delivering incident light to the surface. Distance between the delivering fiber and iris surface is 12 mm. Diameter of the illuminated area is about 5 mm. The collecting fiber is mounted at angle of  $20^\circ$  regarding to central fiber. Distance between tip of collecting fiber and iris surface is 20 mm and, in this geometry, light has been collected from area with diameter about 8 mm. The spectrometer was calibrated using white slab  $\text{BaSO}_4$  with a smooth surface.

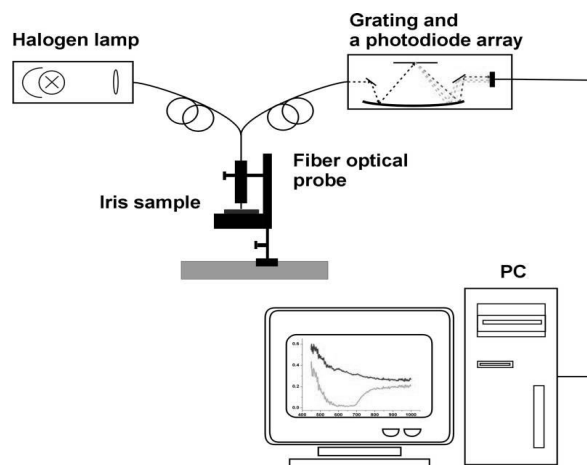


Fig. 6. Experimental setup for in vitro measurements

Experimental setup for registration of digital images of human eye irises is presented in figure 7. For registration of the color images the digital camera Olympus C-5060 (Japan) was used. Its parameters: 5,100,000 effective pixels, Olympus lens from 5.7 mm to 22.9 mm. During the shoot maximum rating aperture value equals to f3.3. Focal length 11.5 was used. The distance between eye and camera objective was 3 cm.



Fig. 7. Experimental setup for *in vivo* registration of digital images of human irises

For the investigation, the special facial fixer (for a chin and a forehead) has been made. It included a mobile part, which supports a chin and moves up - downwards with manual screw rotation. Such equipment needed to be enforced by two lighting elements. Lighting elements were fixed on a movable basis that allowed adjusting the intensity of illumination during the measurements. Digital camera was attached to the vertical holder fixed to movable basis that could be described as a movable device with ability to move in all directions according to the tool stage. Camera can be shifted with fixed steps. It allowed us to carry out shooting of each eye separately in super macro mode with manual focusing. Shooting was done at constant light exposure, which was registered by metering-tool. In fig. 8 digital images of healthy human iris and human eyes with primary open angle glaucoma are presented.

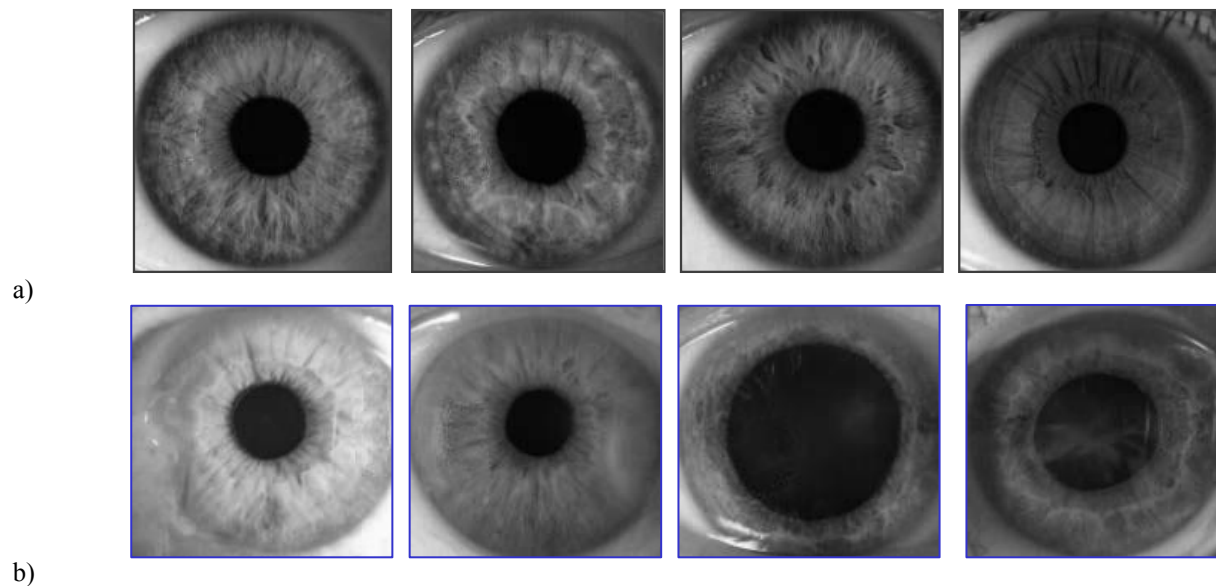


Fig. 8. Digital *in vivo* images of (a) healthy and (b) primary open angle glaucoma human eyes

To process the images of the iris the special computer program has been developed. The base image was separated in three color matrixes of red, green, and blue components. As a result, the averaged scans of the iris image for separated color components (red, green, and blue) corresponding to three spectral ranges for reflectance measurements have been obtained. The brightness of images of the studied irises and test-objects are expressed in units from 0 to 256.

With the special markers the square form area is cut out from the received image (containing an iris of the eye) in which the circle is entered. Then nearby sclera sites are cut, the markers determine the center pupil area, which are deleted. Fig. 9 shows the main steps of image processing.

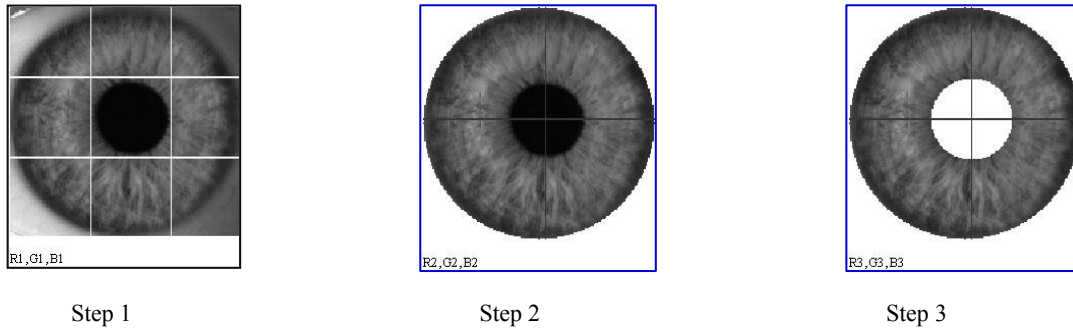


Fig. 9. The main steps of image processing

The image decomposed into R, G, B color coordinates in each pixel. As a reference, a white-test object has been used. For each pixel the measured R, G, B values have been normalized to RGB values of the test object. The obtained reflectance values have been averaged for the whole investigated area. See fig. 9 step 3.

For estimation of melanin content in an iris of human eye the algorithm based on the inverse Monte Carlo technique has been developed. In the framework of the algorithm the following assumptions have been made:

- 1) The iris is presented as a two-layer plane-parallel slab with thickness 460 mm. The deep layer is IPE (10 μm thick) and the upper layer is the iris stroma (450 μm thick).
- 2) The optical properties of the IPE and melanin are presented above.
- 3) Optical properties of iris stroma (for vitiligo samples) have been estimated using the inverse Monte Carlo technique and the result has been presented below.
- 4) Melanin concentration is the variable.

Based on the presented two-layer iris model, the iris diffuse reflectance has been calculated by Monte Carlo technique in the spectral range 400-750 nm. Then the spectrum has been recalculated in color coordinates with the relations

$$R = \int \bar{r}(\lambda) P_0(\lambda) R(\lambda) d\lambda$$

$$G = \int \bar{g}(\lambda) P_0(\lambda) R(\lambda) d\lambda$$

$$B = \int \bar{b}(\lambda) P_0(\lambda) R(\lambda) d\lambda$$

where  $R(\lambda)$  is the iris reflectance, and  $\bar{r}(\lambda)$ ,  $\bar{g}(\lambda)$ , and  $\bar{b}(\lambda)$  is a specific color coordinate,  $P_0(\lambda)$  is spectrum of light source. The calculations have been performed for each pixel. Melanin concentration is varied until color coordinates obtained from the calculations, and color decomposition of experimentally obtained iris images has not been matched. Due to the complex structure of the investigated tissue and simplicity of the presented model, melanin concentration obtained for each spatial coordinate has been averaged throughout iris area.

#### 4. RESULTS AND DISCUSSION

Figure 10 shows reflectance spectra of rabbit irises.

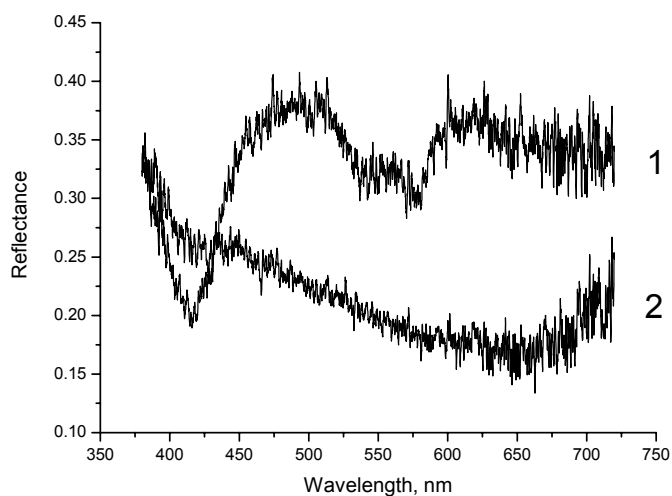


Fig. 10. The typical reflectance spectra of rabbit irises. 1 - the reflectance spectrum of vitaligo iris; 2 - the reflectance spectrum of brown iris of a rabbit.

Using the inverse Monte Carlo technique and taking into account geometry of the measurement optical properties of bloodless vitaligo iris stroma have been estimated. The result is presented in figures 11 and 12. Proceeding from the given technique based on measurement of reflectance, it is possible to estimate the melanin content in an iris of an eye.

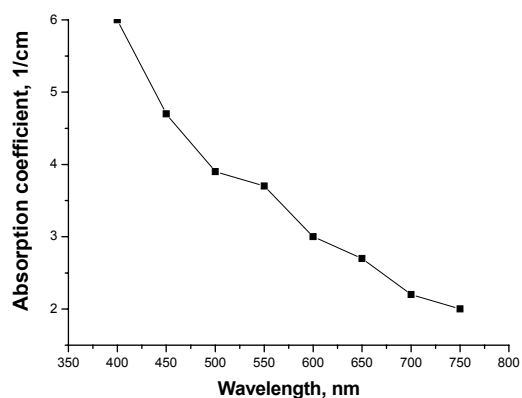


Fig. 11. The absorption properties of bloodless vitaligo iris stroma

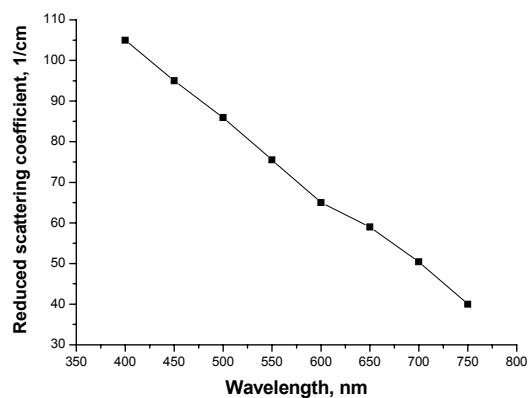


Fig. 12. The scattering properties of bloodless vitaligo iris stroma

In tables 1 and 2 the results of digital image analysis using a designed computer program are respectively presented for healthy volunteers and for volunteers with primary open angle glaucoma.

Table 1. Results of digital image analysis of healthy volunteers

Volunteer (iris color)	R <sub>RGB</sub>	G <sub>RGB</sub>	B <sub>RGB</sub>	Melanin concentration in the iris, mg/ml
0 (blue)	136 (40.8)	112.6 (31)	84.3 (22.3)	2.2 (1.1)
1 (brown)	126.6 (39.3)	62.6 (18.8)	15.5 (2.7)	2.5 (1.1)
2 (blue)	121.4 (14.9)	84.4 (8.7)	44.6 (2.9)	2.5 (0.4)
3 (green)	106.1 (26.5)	74.2 (20)	30.9 (17.9)	3.0 (0.8)
4 (blue)	114 (5.1)	102.3 (3.8)	90.3 (4.1)	2.7 (0.2)
5 (blue)	99.8 (5.6)	81.3 (6)	67.2 (7.8)	3.1 (0.2)
6 (green)	88.7 (3.7)	76.8 (4.3)	65.8 (8.8)	3.5 (0.4)
7 (brown)	71 (4.9)	43.9 (1.7)	19.4 (1.4)	4.3 (0.2)
8 (brown)	177.7 (7.1)	101.1 (3.4)	26.1 (7.8)	1.2 (0.3)
9 (blue)	112.9 (34.1)	85.4 (25.3)	53.5 (17.8)	2.8 (1.4)
10 (green)	118.8 (24.6)	83.5 (15.6)	30.4 (10.9)	2.6 (0.6)
11 (brown)	116.3 (8.3)	71.3 (7.3)	12.8 (5.4)	2.6 (0.2)
12 (blue)	105.4 (17.4)	84.6 (12.9)	58.3 (10.7)	2.9 (0.6)
13 (green)	110.8 (5.7)	70.7 (3.6)	20.3 (4)	2.8 (0.2)
14 (brown)	77.6 (6.4)	39.7 (3.1)	8.6 (2.6)	3.9 (0.3)
15 (blue)	124.4 (17.7)	105.6 (17.5)	86.2 (18)	2.4 (0.5)
16 (blue)	128.9 (16.1)	111.8 (12.9)	95.8 (9.1)	2.3 (0.4)
17 (brown)	87 (24.4)	47.7 (10.6)	8.4 (1.4)	3.7 (1.0)
18 (green)	146.8 (28.1)	88.7 (18.4)	22 (9.8)	1.9 (0.7)
19 (green)	112.7 (16.2)	71.6 (5.7)	22 (3.7)	2.7 (0.5)

Table 2. Results of digital image analysis of patients with open angle glaucoma

Patient (iris color)	R <sub>RGB</sub>	G <sub>RGB</sub>	B <sub>RGB</sub>	Melanin concentration in the iris, mg/ml
1 (brown)	129 (11.2)	59 (6.1)	6 (1.4)	2.3 (0.3)
2 (blue)	116.3 (7.6)	71.5 (5.9)	20.4 (9)	2.6 (0.2)
3 (blue)	122.9 (16.2)	76.3 (10.7)	14.9 (5.8)	2.4 (0.5)
4 (brown)	130.5 (14.5)	59.8 (8.6)	6 (2.3)	2.3 (0.4)
5 (blue)	119.6 (7.6)	74 (10.1)	26.9 (23.9)	2.5 (0.2)
6 (blue)	128.6 (10.7)	81.7 (7.3)	30.4 (12.7)	2.3 (0.3)
7 (blue)	136.4 (8.5)	115.4 (8.1)	98.6 (9.3)	2.1 (0.2)
8 (green)	137.2 (18.5)	83 (6.9)	24.4 (9.6)	2.1 (0.3)
9 (green)	181.7 (39.4)	117.7 (36.9)	48.7 (34.8)	1.2 (0.8)
10 (blue)	98.3 (15.3)	81.5 (14.4)	66.5 (14.9)	3.2 (0.5)
11 (blue)	113.3 (14.2)	97.6 (11.8)	85.3 (13.2)	2.7 (0.4)
12 (brown)	128.8 (11.8)	58.3 (6.5)	9.5 (3)	2.3 (0.3)

In tables 3 and 4, the data, averaged from tables 1 and 2 are presented. From table 3 it is seen that maximal melanin concentration has been obtained for brown eyes. For blue and green eyes the melanin content is smaller.

Table 3. Mean melanin concentration in healthy human iris measured *in vivo* (from digital analysis of color images)

Color of eyes	Melanin concentration, mg/cm <sup>3</sup>
blue eyes	26.2±3.4
brown eyes	30.3±11.7
green eyes	27.4±5.4

Table 4 Mean melanin concentration in human iris with glaucoma measured *in vivo* (from digital analysis of color images)

Color of eyes	Melanin concentration, mg/cm <sup>3</sup>
blue eyes	25.5±3.6
brown eyes	22.5±0.2
green eyes	16.1±6.4

From table 4 it is seen that maximal melanin concentration is observed for blue eyes in contrast to data of table 4. In



irises of eyes with glaucoma the mean content of melanin is less in comparison with one in irises of healthy eyes. The major difference was obtained for brown and green color eyes.

## ACKNOWLEDGMENTS

The research described in this publication has been made possible, in part, by grants PG05-006-2 and REC-006 of U.S. Civilian Research and Development Foundation for the Independent States of the Former Soviet Union (CRDF) and the Russian Ministry of Science and Education, grant of the Russian Federal Agency of Education Russian Federation 1.4.06, and grant of RFBR No. 06-02-16740-a. The authors thank Dr. S.V. Eremina (Department of English and Intercultural Communication of Saratov State University) for the help in manuscript translation to English.

## REFERENCES

1. V.V. Tuchin, *Tissue Optics: Light Scattering Methods and Instruments for Medical Diagnosis*, SPIE Press, TT38, Bellingham, USA, 2000.
2. N.B. Shulpina, *Biomicroscopy of the eye*, Moscow, 1972.
3. M.L. Berliner, *Biomicroscopy of the eye*, in *Slit-lamp microscopy of the living eye*, New York, p. 9-14, 1949.
4. M Zaltsmann, *Anatomy and histology of the human eye in normal, its development and withering*, Moscow, 1913.
5. E.S. Velhover, V.F. Ananin, *Clinical iridology*, Moscow, 1992.
6. E.S. Velhover, *Iridology*, Moscow, 1992.
7. A.M. Vodovozov, A.A. Ribnikov, *Estimation iris of the eye in transformed light*, Moscow, 1992.
8. V.V. Kononov, A.A. Antonov, *Practical iridology*, 1990.
9. A.J. Samoilov, Iris of an eye, in *Big Medical Encyclopedia*, **27**, 842-849, 1962.
10. A.J. Samoilov, Choroid of an eye, in *Big Medical Encyclopedia*, **30**, 953-956, 1963.
11. D.A. Enikeev, S.A. Lobanov, *Iridoallopastic*, 1996.
12. E.V. Bobrova, "Ultrastructure of human eye dilator," in *Some questions of experimental and clinical medicine*, 22-25, Moscow, 1977.
13. E.V. Bobrova, A.V. Petrov, "Ultrastructure of the front layers and pupill dilator of an human eye iris," *Bullen of Ophthalmology*, **4**, 33-36 (1978).
14. V.N. Alekseev, I.A. Samusenko, "Clinical-morphological changes in the forward piece of the eye at experimental glaucoma," *Glaucoma*, **1**, a80 (2004).
15. M. Hammer, D. Schweitzer, "Quantitative reflection spectroscopy at the human ocular fundus," *Phys. Med. Biol.*, **47**, 179-191 (2002).
16. F.C. Delori, K.P. Pflibsen, "Spectral reflectance of the human ocular fundus," *Appl. Opt.*, **28**, 1061-1077 (1989).
17. S.L. Preece, E. Claridge, "Monte Carlo modelling of the spectral reflectance of the human eye," *Phys. Med. Biol.*, **47**, 2863-2877 (2002).
18. P.D. Imesch, I.H.L. Wallow, D.M. Albert, "The color of the human eye: A review of morphologic correlates and of some conditions that affect iridial pigmentation," *Survey of Ophthalmol.*, **41**, 117-123 (1997).
19. T.P. Dryja, M. O'Neil-Dryja, D.M. Albert, "Elemental analysis of melanins from bovine hair, iris, choroid, and retinal pigment epithelium," *Invest. Ophthalmol. Visual Sci.*, **18**, 231-236 (1979).
20. E. Buszman, R. Rozanska, "Interaction of thioridazine with ocular melanin *in vitro*," *Acta Pol Pharm.*, **60**(4), 257-61 (2003).
21. M. Hammer, D. Schweitzer, E. Thamm, A. Kolb, "Non-invasive measurement of the concentration of melanin, xanthophyll, and hemoglobin in single fundus layers *in vivo* by fundus reflectometry," *Int. Ophthalmol.*, **23**(4-6), 279-89 (2001).
22. S. Peters, U. Schraermeyer, "Characteristics and functions of melanin in retinal pigment epithelium," *Ophthalmology*, **98**(12), 1181-1185 (2001).
23. M. Braun, A. Kage, K. Heimann, U. Schraermeyer, "Retinal pigment epithelial cells from Royal College of Surgeons dystrophic rats can take up melanin granules," *Graefes Arch Clin Exp Ophthalmol.*, **237**(1), 67-71 (1999).
24. S. Jacques, Published on the personal web-site: [www.omlc.ogi.edu](http://www.omlc.ogi.edu).
25. M. Hammer, A. Roggan, D. Schweitzer, G. Muller, "Optical properties of ocular fundus tissues – an *in vitro* study using the double-integrating-sphere technique and inverse Monte Carlo simulation," *Phys. Med. Biol.*, **40**, 963-978 (1995).